

Switchable reflectivity on silicon from a composite VO₂-SiO₂ protecting layer

R. Lopez,^{a)} L. A. Boatner, and T. E. Haynes

Condensed Matter Sciences Division, Oak Ridge National Laboratory, Oak Ridge, Tennessee 37831

R. F. Haglund, Jr. and L. C. Feldman

Department of Physics and Astronomy and Vanderbilt Institute of Nanoscale Science and Engineering, Vanderbilt University, Nashville, Tennessee 37235

(Received 23 April 2004; accepted 18 June 2004)

Surfaces whose reflectivity can be thermally controlled were formed on single crystals of silicon by using ion beams to create a nanocomposite layer consisting of VO₂ precipitates embedded in a thin-film matrix of amorphous SiO₂. The surface nanocomposite layer was produced by first thermally oxidizing a Si crystal to produce an overlying SiO₂ film with a desired thickness. Stoichiometric coimplantation of vanadium and oxygen ions and subsequent thermal processing were then employed to form embedded VO₂ nanoparticles in the SiO₂ film. The reflectivity of the vanadium dioxide particles undergoes large changes at the VO₂ semiconductor-to-metal phase transition, thereby providing the mechanism for thermally controlling the reflectivity of the VO₂/SiO₂/Si layer and, effectively, the Si crystal surface. The VO₂/SiO₂ nanocomposite layer was applied in a device configuration in which heating via current through the Si substrate is used to control the surface reflectivity. © 2004 American Institute of Physics. [DOI: 10.1063/1.1784546]

Vanadium dioxide (VO₂) is one of a number of transition-metal oxides that undergo either an insulator-to-metal or semiconductor-to-metal transition at a characteristic phase-transition temperature. Following the early observations of Morin,¹ the physical properties of various oxides of vanadium have been extensively investigated in the region of their phase transitions. In particular, the semiconductor-to-metal phase transition temperature of VO₂ ($T_c \sim 68^\circ\text{C}$) falls in a convenient range—making VO₂ a popular system for exploring the physical mechanisms behind phenomena of this type. On cooling through the phase transition, VO₂ undergoes a first-order structural change from a high-temperature, metallic tetragonal rutile phase to a low-temperature monoclinic, semiconducting form. Correspondingly, the electrical and optical properties of VO₂ undergo significant and abrupt changes across this structural phase transition. The metallic properties of the high-temperature VO₂ phase strongly enhance the reflection of incident light at near-infrared frequencies;² while the low-temperature phase is a narrow band-gap semiconductor³ with a relatively high transparency in the same infrared spectral region. It is precisely this near-room-temperature transition and the associated large optical and electronic property changes that make VO₂ a candidate material for a wide variety of technological applications, such as thermochromic coatings,⁴ optical and holographic storage,^{5,6} fiber-optical switching devices,⁷ laser scanners,⁸ missile training systems,⁹ and ultrafast optical switching.¹⁰

In the present work, near-surface nanocomposites with a thermally variable reflectivity were produced on single-crystal Si by using ion beams and thermal processing to form small VO₂ precipitates embedded in a thermally grown overlying SiO₂ layer. This nanocomposite-film/Si-crystal system

was subsequently employed in a device configuration where resistive heating using current applied to the Si crystal substrate caused the VO₂/SiO₂ nanocomposite temperature to vary and thereby to control the reflectivity. This configuration is also capable of operating in a “smart” mode in which sufficiently intense incident light that is directly absorbed by the embedded VO₂ nanoparticles results in heating that drives the particles into the metallic phase and thus increases the reflectivity of the VO₂/SiO₂/Si crystal surface.

In order to form variable-reflectivity surfaces on Si, amorphous SiO₂ layers were initially grown on device-quality silicon single-crystal wafers by conventional annealing for a controlled amount of time in an oxidizing atmosphere. The annealing time was adjusted to produce a silicon oxide film with a nominal thickness of ~ 200 nm. The general characteristics of the phase-transition properties of VO₂ nanoparticles formed by ion-beam methods in bulk amorphous SiO₂ were described previously, and one particularly noteworthy feature is the unusually large hysteresis (up to $\sim 45^\circ\text{C}$ in width) exhibited by VO₂ particles formed in bulk silica hosts.¹¹ In the present case of VO₂ nanoparticle formation in a thin silicon oxide layer grown on a Si single-crystal substrate, the SiO₂ surface layer was coimplanted at room temperature with vanadium and oxygen ions at energies of 100 and 36 keV, respectively. These implantation energies, which were calculated using the computer code TRIM,¹² were selected to ensure the superposition of both the vanadium- and oxygen-implant distributions halfway through the amorphous SiO₂ layer. The vanadium-ion implantation doses ranged from 0.5 to 1×10^{17} ions/cm² and were combined with oxygen-implant doses in the stoichiometric proportion of 1:2 for the formation of VO₂. Subsequent to the ion coimplantation, the formation of the VO₂ precipitates on the SiO₂ film was accomplished by thermally annealing the V and O coimplanted specimens in flowing argon at atmospheric pressure and at $T = 1000^\circ\text{C}$ for 10 min. In carrying out this final step, the annealing furnace was first preheated to the desired

^{a)}Author to whom correspondence should be addressed; also at: Department of Physics and Astronomy, 6301 Stevenson Center, Vanderbilt University, Nashville, TN 37235; electronic mail: rene.lopez@vanderbilt.edu

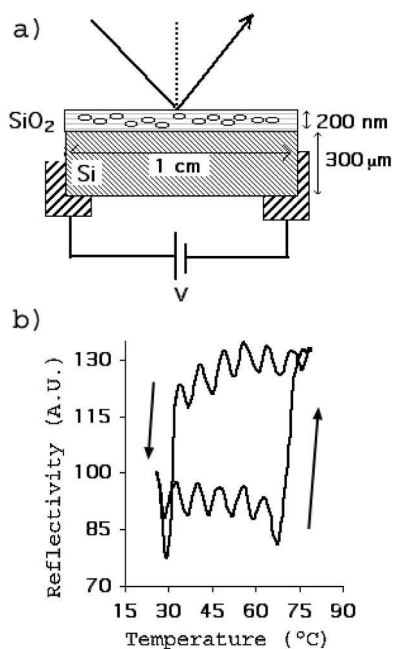


FIG. 1. (a) Schematic of the silicon-based variable reflectivity system employing electrical connections to allow the silicon substrate to be used as a heat source for switching the VO₂ nanoparticles between the semiconducting and metallic phases. (b) Temperature response of the reflectance showing the VO₂ precipitate phase transition and associated hysteresis curve plotted using the configuration shown in (a) and determined using 1.5 μm light from a HeNe laser incident at an angle of 25° relative to the surface normal. The 200-nm-thick SiO₂ film was coimplanted with 0.5×10^{17} V ions/cm² at 100 keV and 1.0×10^{17} O ions/cm² at 36 keV, and annealed for 10 min at 1000°C in flowing argon.

temperature and then evacuated to a pressure of 5×10^6 Torr prior to introducing the high-purity argon and establishing a constant gas flow.

The VO₂-nanoparticle/SiO₂-film/Si-crystal samples were characterized using Rutherford backscattering spectrometry (RBS), x-ray diffraction (XRD), and infrared optical reflection. Atomic concentration profiles of the V and O that were coimplanted into the SiO₂ layer were compared before and after the VO₂ precipitation step by using the RBS analysis. The RBS results showed that the distribution “in depth” of the vanadium ions following the annealing step was totally confined inside the SiO₂ layer, and no effects of any vanadium segregation to the surface were observed. The VO₂ precipitate formation was directly established by XRD studies made at the CuK_α wavelength. The results of a θ -2 θ scan show a single Bragg reflection at $2\theta=27.81^\circ$ that is assigned to the (011) reflection of the monoclinic phase of embedded VO₂ crystals. The general dependence of the VO₂ particle size and morphology on the thermal processing conditions for an amorphous SiO₂ host has previously been described in detail.¹³

Due to the complex oxidation behavior of vanadium, the most definitive confirmation of the formation of VO₂ is via an observation of the semiconductor-to-metal phase transition in the critical temperature region that is characteristic of VO₂. In order to carry out surface-reflectivity observations of the phase-transition characteristics of VO₂ precipitates embedded in an amorphous SiO₂ film, the device configuration illustrated in Fig. 1(a) was fabricated. In this case, electrical contacts are applied directly to the silicon substrate, which was then used as a controlled resistive heating source by

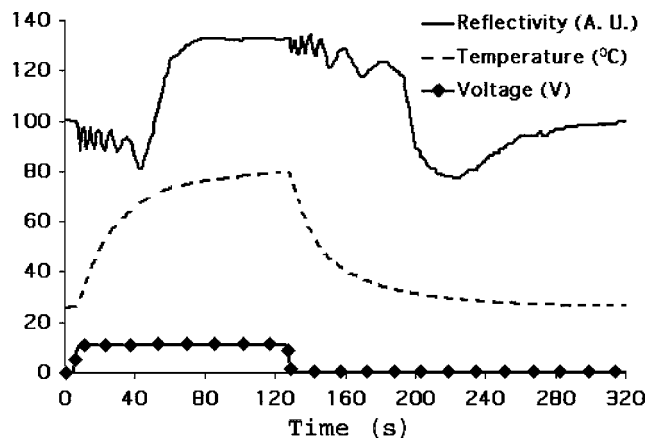


FIG. 2. Temperature, reflectivity, and applied voltage as a function of time for the sample shown in Fig. 1(a). The temporal response of the system is determined by the Si-substrate thermal and electrical properties and the input power and not by the intrinsic switching time of the VO₂ particles embedded in the SiO₂ film.

simply applying a variable dc voltage. The sample temperature was measured with a precision thermocouple placed in direct contact with the SiO₂ layer that contained the VO₂ particles. Given the size of the Si substrate employed ($\sim 10 \times 10 \times 0.3$ mm³ and its resistivity $\sim 0.1 \Omega$ cm), a voltage of 11 V was required to overcome the convection cooling and heat the VO₂/SiO₂ composite film to a temperature above the T_c for VO₂. Figure 1(b) shows the hysteretic reflectivity response of the VO₂ precipitate phase transition determined using this configuration with light from a 1.5 μm HeNe laser incident at an angle of 25°. As shown in Fig. 1(b), the reflectance increases when the sample is heated above 70°C, and a respective reversal to the original state occurs when the system is subsequently cooled below 35°C. This increase in reflectance is expected from the metallic behavior of the high-temperature phase.

In Fig. 1(b), we also observe the series of small modulations that are superimposed on the large reflectivity change arising from the phase transition in the VO₂ precipitates. These small modulations are independent of the large negative excursions in reflectivity at the low- and high-temperature end of the hysteresis loop. The small modulations are apparently the result of the thermal expansion of the silicon substrate as the temperature varies, and hence the thickness, of the Si substrate is varied. At 1.5 μm, Si is quite transparent, but its refractive index is 3.48; the index of refraction of the silica overlayer is 1.44 at this wavelength. The modulation of the reflectivity from the sample is due to interference between the light rays undergoing direct reflection from the SiO₂ surface and those that pass through the SiO₂ to the underside of the Si substrate and are then reflected back through the SiO₂. In fact, this feature is observed in reflectivity measurements made on the bare Si substrate. The calculated fringe contrast in the total reflected signal agrees well with the thickness and optical constants of the P-doped silicon wafer ($\sim 0.3 \Omega$ cm), however, the expansion coefficient would have to be slightly larger than pure Si, in order to account for all the observed oscillations in this temperature range.¹⁴ What is not accounted for at the present time are the two large dips in reflectivity at the beginning and end of the hysteresis loop. While Mie scattering could certainly change the overall intensity of the measured signal, it is difficult to

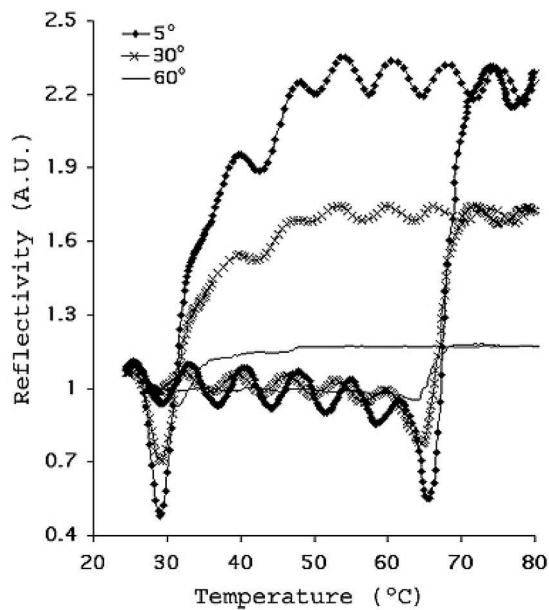


FIG. 3. Dependence on the angle of incidence of the optical reflectance change due to the phase transition of embedded VO_2 precipitates in a 200-nm-thick SiO_2 layer formed on a Si single-crystal substrate. The large ($\sim 35^\circ$ -wide hysteresis) is characteristic of VO_2 particles formed in an amorphous SiO_2 host. The sample was coimplanted with 1.0×10^{17} V ions/cm² at 100 keV and 2.0×10^{17} O ions/cm² at 36 keV, and annealed for 10 min at 1000°C in flowing argon.

see how these signals could be coherent with the specular reflection. Accordingly, this particular feature must be regarded as an unresolved issue at the present time.

Figure 2 illustrates the time response of the surface reflectivity and temperature along with the time variation of the applied voltage for the variable-reflectivity device configuration shown in Fig. 1(a). Since in this case, the silicon substrate is being used as a resistive heater, the time response is determined primarily by the Si substrate heat capacity, its resistivity, and the magnitude of the applied dc voltage. These thermal and input-power parameters are limiting the time response of this device since the VO_2 particles are capable of switching from the semiconducting to the metallic state at very high rates. The reflectance change (normalized with respect to the semiconductor state at $T=25^\circ\text{C}$) is shown in Fig. 3 for several angles of incidence of the 1.5 μm HeNe laser. The relative magnitude of the change in reflectivity

versus the angle of incidence is quite large, and it is explained by observing that at large angles, the Fresnel reflectance is larger than the transmittance in all the interfaces; in particular, the air/ SiO_2 : VO_2 interface will reduce the amount of light actually entering the structure and interacting with the VO_2 . Therefore, the effective switching gets smaller. This is clearly an important variable affecting the magnitude of the optical switching. The relatively large switching magnitude of the IR reflectivity makes these VO_2/SiO_2 nanocomposite films of interest for use as “smart” self-limiting devices for protecting an underlying silicon wafer from overheating due to incident infrared radiation (e.g., as in the case of photovoltaic solar cells in nonterrestrial environments).

The authors thank Pam H. Fleming for providing the oxidized silicon wafer samples and the staff at the former Surface Modification and Characterization Research Facility at ORNL for their technical support. This research was supported in part by the Office of Science, U.S. Department of Energy through a grant to Vanderbilt University (NSET Grant No. DE-FG02-01-ER45916) and by the Laboratory Directed Research and Development Program of Oak Ridge National Laboratory, which is managed by UT-Battelle, LLC, for the U.S. Department of Energy under Contract No. DE-AC05-00OR22725.

¹F. J. Morin, Phys. Rev. Lett. **3**, 34 (1959).

²P. J. Hood and J. F. Natale, J. Appl. Phys. **70**, 376 (1991).

³B. Felde, W. Neissner, D. Schalch, A. Sharmann, and M. Werling, Thin Solid Films **305**, 61 (1997).

⁴C. G. Granqvist, Phys. Scr. **32**, 401 (1985).

⁵M. Fukuma, S. Zembutsu, and S. Miyazawa, Appl. Opt. **22**, 265 (1983).

⁶W. R. Roach, Appl. Phys. Lett. **19**, 453 (1971).

⁷C. E. Lee, R. A. Atkins, W. N. Giler, and H. F. Taylor, Appl. Opt. **28**, 4511 (1989).

⁸J. S. Chivian, W. E. Case, and D. H. Rester, IEEE J. Quantum Electron. **15**, 1326 (1979).

⁹M. A. Richardson and J. A. Coath, Opt. Laser Technol. **30**, 137 (1998).

¹⁰M. F. Becker, A. B. Buckman, R. M. Walser, T. Lepine, P. Georges, and A. Braun, J. Appl. Phys. **79**, 2404 (1996).

¹¹R. Lopez, L. A. Boatner, L. C. Feldman, R. F. Haglund, Jr., and T. E. Haynes, Appl. Phys. Lett. **79**, 3161 (2001).

¹²J. F. Ziegler, *Transport and Range of Ions in Matter*, Ver. 96.01 (IBM Research, Yorktown Heights, NY, 1996).

¹³R. Lopez, T. E. Haynes, L. A. Boatner, L. C. Feldman, and R. F. Haglund Jr., J. Appl. Phys. **92**, 4031 (2002).

¹⁴M. Born and E. Wolf, *Principles of Optics*, 7th ed. (Cambridge University Press, Cambridge, 2002).